

## Design and Implementation of Iterative Learning Control for an Electro-Hydraulic Servo System

Naveen C<sup>1\*</sup>, Meenakshipriya B<sup>1</sup>, Sathiyavathi S<sup>1</sup> & Tony Thomas A<sup>2</sup>

<sup>1</sup>Department of Mechatronics Engineering, Kongu Engineering College, Erode 638 060, Tamil Nadu, India

<sup>2</sup>Department of Mechatronics Engineering, KCG College of Technology, Chennai 600 097, Tamil Nadu, India

*Received 14 January 2022; revised 24 November 2022; accepted 17 April 2023*

In order to produce an accurate movement of double-acting hydraulic cylinder of the Electro-Hydraulic Servo System (EHSS), an Iterative Learning Controller (ILC) approach is implemented in this work. Nonlinearity and imprecision occurs in the hydraulic systems because of friction. Traditional controllers are incapable of providing effective control performance throughout the entire operating range and insufficient to handle repetitive task. To manage the repetitive task, a memory-based learning control analysis is suitable. This research focuses to construct the ILC for governing the servo spool valve, which is responsible for the hydraulic cylinder displacement. The proposed ILC consists of learning filter, learning gain and robustness filter. Proportional, Integral and Derivative (PID) controller is devised to validate the outcome of ILC. Controllers are constructed based on the system modelling. The effectiveness of the suggested controller is shown through simulation and experimental findings. ILC provides an average of 50% minimal overshoot and settles 7 sec before the PID controller is designed. Due to model uncertainty, PID controller results 0.2 sec better rise time than ILC. In ILC's architecture objective function is designed to achieve minimal overshoot and quick settling of hydraulic cylinder. So, no consideration is given to the error indices. These findings will help hydraulic stamping application, which requires the accurate displacement of piston to avoid damage of work piece. These results show that the proposed controller achieves desired outcome displacement of hydraulic cylinder.

**Keywords:** Closed loop control, Double acting hydraulic cylinder, Position control, Proportional integral derivative controller, Servo spool valve

### Introduction

An EHSS is made up of an electrically driven servo valve that regulates the hydraulic fluid fed to a cylinder. Because of their solidity, sturdiness, capability to withstand massive inertia, and stability, it is commonly employed in versatile heavy-duty applications.<sup>1</sup> EHSS are used in the following application such as Autonomous tractor, Half car active suspension system, Metal bar cropping and Hydraulic press.<sup>2-5</sup> Meanwhile, it has downsides that include external disturbances, aging, leakage and flow saturation of valve. These issues can be fixed by implementing a closed-loop controller and also the displacement precision can be increased even under harsh conditions.<sup>1</sup> For servo valve-based applications, many control systems have been applied, which includes model-based and non-model-based control. In the Model-based control, the efficiency, stability and accuracy are improved by using system dynamics. PID is employed in many application

because of its design simplicity.<sup>6</sup> Sliding Mode Controller (SMC) performs better on nonlinearity and disturbances.<sup>1</sup> Zero Phase Error Tracking Controller (ZPETC) improves error tracking and response smoothness.<sup>7</sup> Internal Model Controller (IMC), Model Predictive Controller (MPC), Adaptive Back-Stepping Controller (ABS) and Iterative Learning Controller (ILC) has been implemented with some standard assumption and ignorance to achieve the desired response.<sup>8-11</sup> However, it's difficult to identify the accurate mathematical model of EHSS due to large number of model uncertainties such as external disturbances and leakages. To find the system parameters, non-model-based control procedures are employed. It's also flexible and adaptable for modification of rules. Non-model based control strategies like Fuzzy Iterative Learning Control (FILC), the error correction in each cycle is improved.<sup>5</sup> To address complex optimization issues, the PID type Genetic Algorithm (GA) is applied.<sup>12</sup> For applications involving categorization and retrogression, neural networks are investigated.<sup>13</sup>

\*Author for Correspondence  
E-mail: cnaveen@kongu.ac.in

Hybrid neural-genetic algorithm improves the precision of nonlinear systems and the Particle Swarm Optimization (PSO) reduces the computing time required for system parameter identification.<sup>14</sup> To solve large-scale optimization problems, the Genetic Algorithm is applied to potentially facilitate the applications of the EHSS.<sup>15</sup> An iterative learning mechanism is used in complex gait simulation process to maneuver Electro-hydraulic Loading System into a position trajectory that closely resembles the desired curve.<sup>16</sup>

Performance of EHSS has been tested with both the learning and non-learning control schemes. The non-learning controllers may not be sufficient when there are significant environmental and plant-related uncertainties. Conventional controllers no longer offer appropriate and attainable control performance across the whole operating range, because finite-time tracking control is challenging with the usage of conventional controllers. The learning controller makes use of the error signal data from the prior cycle. It features a memory component that keeps track of the signal from the previous repetition and acts on it. Non-learning controllers are used for non-repetitive activities. It integrates few system-restrictive circumstances. Based on the complexity in system model, suitable control strategy can be implemented to improve the resistance to system uncertainty and disruptions.

To achieve a high level of precision, especially for a repeating task, ILC has been implemented.<sup>17,18</sup> Learning from earlier iterations, ILC improves the system's performance. Learning controller offers better results by utilizing the information of earlier iteration error signals, but a non-learning controller ignores them.<sup>19</sup> ILC updates the present trial input with data from prior trials, allowing performance to increase over time. ILC is best for operations that repeat the same task over a set period of time.<sup>20</sup> ILC increases the system performance in manufacturing process such as Additive manufacturing, Computer numerical control machine tool, Cyclic production process and Injection molding process.<sup>21-23</sup> ILC is applied to control the Building temperature, Chemical reactor and Current control for switched reluctance motor.<sup>24-26</sup> ILC implemented in heavy load applications such as Electro-hydraulic Servo System, Gait simulator, Electro-hydraulic metal bar cropping and Gantry robots.<sup>11,16,27,28</sup> ILC is successfully applied in non-repetitive practical applications. It is used to achieve high potential in the non-repetitive pick and

place operation of the delta robot.<sup>29</sup> ILC is implemented in mobile robot to address issues with trajectory tracking when the robot's position is unknown at the beginning of each iteration.<sup>30</sup> In order to obtain accurate position and pressure tracking capabilities as well as resilience, an electro-pneumatic servo system is exposed to an ILC approach with a PID feedback loop.<sup>31</sup> In wafer scanning, ILC improves the performance when the process cycle has distinct phases, where repeated disturbances are less prevalent than non-repetitive disturbances.<sup>32</sup> ILC is also utilized to enhance non-repetitive performance.<sup>33</sup>

### Objective

To construct an iterative learning controller for an EHSS that achieves zero overshoot and fast settling time, as well as to test and verify the system's performance.

### Experimental Setup Details

#### Electro-Hydraulic Servo system (EHSS)

##### Block Diagram of Electro-Hydraulic Servo System (EHSS)

Block diagram of EHSS is shown in Fig. 1. Input block is the set point, Controller is used to regulate the displacement, and Feedback is the signal which carries the displacement information of hydraulic cylinder, Data Acquisition Card (DAQ) is employed to communicate with the programming device and hardware. Linear Variable Differential Transformer (LVDT) senses the position of hydraulic cylinder and electro hydraulic power pack stores the fluid which is used as a power medium.

##### Photography of Electro-hydraulic Servo System

Photograph of an EHSS is displayed in Fig. 2. DAQ is used to facilitate communication between Personal computer and EHSS. DAQ is equipped with

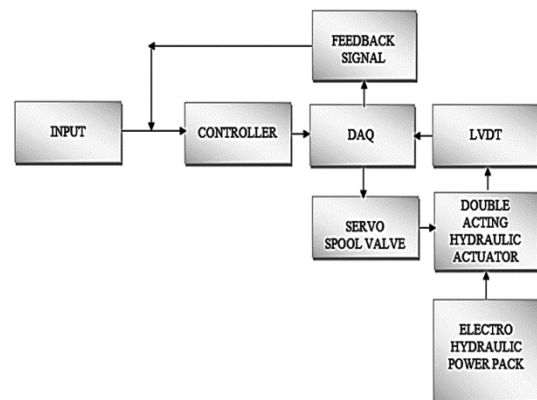


Fig. 1 — Block diagram of EHSS



Fig. 2 — Photography of EHSS: 1-Personal computer (PC), 2-DAQ, 3-Hydraulic power pack, 4-Three phase fixed displacement pump, 5-Double-acting hydraulic cylinder, 6-Pressure gauge, 7-LVDT, 8-Accumulator, 9-Servo spool valve

Analog to Digital Converters (ADC) and Digital to Analog Converters (DAC). LVDT senses the displacement of double-acting hydraulic cylinder and the analog signal reaches the ADC. DAC acquires the digital controller signal from controller and turns it into an analog signal that is sent to the servo spool valve. Three phase fixed displacement pump is used to generate hydraulic power for hydraulic systems. Accumulator and pressure gauge are employed to sense and store the hydraulic power respectively.

The hydraulic cylinder has a stroke length of 250 mm. Displacement is monitored by an LVDT and is operated by a servo valve. The input current controls the spool-valve's displacement. The direction and speed of a piston's movement are determined by the location of the spool-valve. Software for closed-loop control is built using MATLAB. The difference between the set point and obtained signal of displacement is the error signal ( $e$ ). The controller uses the error signal and produces the command signal to regulate the position of hydraulic cylinder.

**Functional Flow Diagram**

Physical connection, fluid flow and electrical connections are shown in Fig. 3. Hydraulic power pack is controlled by a 3-phase power source, which includes a hydraulic sump that is physically connected to a three-phase induction motor. The relief valve receives the fluid flow from the hydraulic sump via the filter and accumulator. Fluid flows from the relief valve to the hydraulic cylinder via the servo valve, with the return fluid returning to the hydraulic sump. To sense the position of the hydraulic cylinder, the LVDT is physically connected to it. An electrical

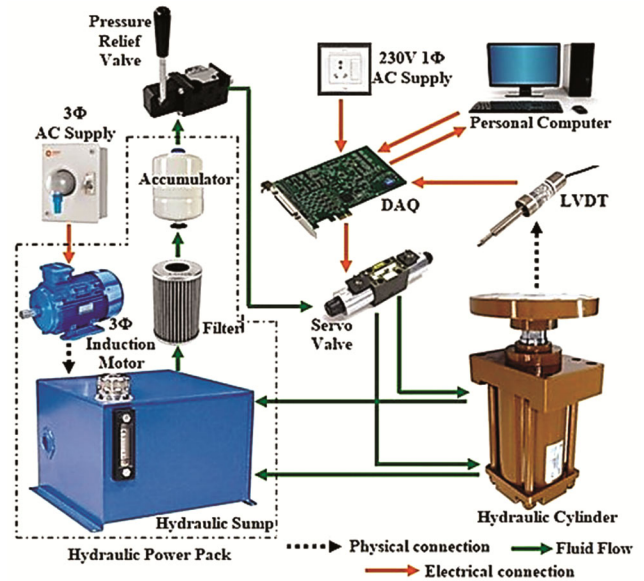


Fig. 3 — Functional flow diagram of EHSS

connection is established between DAQ, personal computer and servo valve.

**System Dynamics**

The mathematical model is derived in order to determine the system transfer function. The kinematics of an EHSS is simplified using following assumptions. i) Ignoring cylinder and valve fluid leaks. ii) Neglecting the piston-cylinder frictional force. iii) Consider that the spool position of the servo valve is critically lapped.

**EHSS Parameters and Its Values**

Coil resistance ( $R$ ) = 20 ohm, Coil inductance ( $L$ ) = 0.05 H, length of cylinder stroke ( $a$ ) = 250 mm, Coefficient of discharge ( $C_d$ ) = 0.7, Area gradient ( $w$ ) = 0.024 m<sup>2</sup>/m, Piston's cross sectional area ( $A$ ) = 0.001855 m<sup>2</sup>, Pressure supply ( $P_s$ ) =  $3.5 \times 10^4$  Pa, Load's damping coefficient ( $b'$ ) = 1200 Ns/m, Density ( $\rho$ ) = 839.612 Kg/m<sup>3</sup>, Mass of the load ( $m'$ ) = 9.5 Kg, Load-spring constant ( $k'$ ) = 410 N/m, Damping coefficient ( $b$ ) = 540 Ns/m, Mass ( $m$ ) = 0.5 Kg, Volume ( $V_o$ ) =  $3.1 \times 10^{-4}$  m<sup>3</sup>, Spring constant ( $k$ ) = 20 N/m.

**Electrical Cylinder and Spool**

The voltage ( $v$ ) applied for an electrical actuation is described using the Current through coil ( $i$ ), Inductance ( $L$ ) and Spool displacement ( $x_v$ ) as follows:

$$v = iR + \frac{L'(\frac{x_v}{(a+x_v)})di}{dt} + \frac{iaL'}{(a+x_v)^2}x_v \quad \dots (1)$$

The Eq. (1) yields current via the coil as

$$\frac{di}{dt} = a + \frac{x_v}{x_v L' \left( v - iR - \frac{iaL'}{(a+x_v)^2} x_v \right)} \quad \dots (2)$$

The magnetic force generated by the coil is used to carry the displacement in the spool plunger. The Eq. (3) relates the spool displacement, flow force and magnetic force.

$$\frac{iaL'}{(a+x_v)^2} = m\ddot{x}_v + b\dot{x}_v + kx_v + 0.43w(P_s - P_L)x_v \quad \dots (3)$$

The spool valve's displacement is calculated using Eq. (3) as follows:

$$\ddot{x}_v = \frac{\frac{iaL'}{(a+x_v)^2} - b\dot{x}_v - kx_v - 0.43w(P_s - P_L)x_v}{m} \quad \dots (4)$$

**Double-Acting Cylinder**

Based on spool displacement, the fluid flow rate (QL) to the cylinder is given as

$$Q_L = C_d w x_v \sqrt{(P_s - \text{sgn} x_v - P_L) / \rho} \quad \dots (5)$$

**Load**

The load is driven by the pressure differential inside the cylinder.

$$AP_L = m' \ddot{X}_L + b' \dot{X}_L + k' X_L \quad \dots (6)$$

$$\ddot{X}_L = \frac{AP_L - b' \dot{X}_L - k' X_L}{m'}$$

The load pressure (PL) and load-displacement (V (t)) are calculated as follows, where β is the bulk modulus

$$\dot{P}_L = \frac{4\beta}{v(t)} (Q_L - A\dot{X}_L)$$

$$V(t) = V_0 + AX_L \quad \dots (7)$$

The system transfer function, often known as the open-loop response, is implemented in MATLAB-Simulink

$$G(S) = \frac{X_v(S)}{v(s)} = \frac{40}{7.5S+1} \quad \dots (8)$$

**Controller Design**

**Iterative Learning Controller**

Learning from prior executions is the foundation of ILC. A system that performs the same task repeatedly will function more effectively as a result. When a disturbance persists, it either rejects or adheres to a certain reference.<sup>7</sup>

Block diagram of Iterative Learning Controller is depicted in Fig. 4. The algorithm's performance is influenced by the robustness filter Q, learning gain K<sub>l</sub>

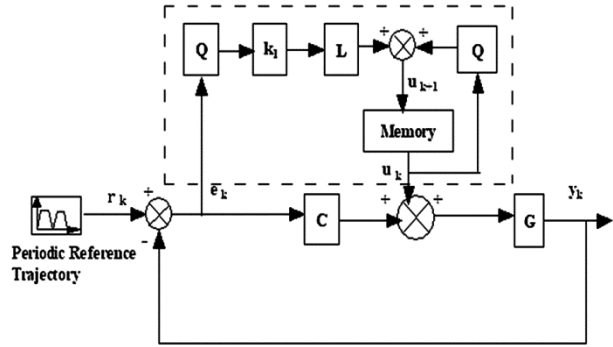


Fig. 4 — Block diagram of iterative learning controller

and learning filter L. The convergence research uses a minimal gain under the consideration that r<sub>k</sub> = 0 and all starting conditions are set as zero.

**Learning Filter (L)**

The error signal e<sub>k</sub> and the feed-forward signal u<sub>k</sub> is related.

From the Fig. 4, error  $e_k = r_k - y_k \quad \dots (9)$

$e_k = -y_k \quad (\because r_k = 0) \quad \dots (10)$

Now, the output y<sub>k</sub>

$$y_k = G (u_k + C e_k)$$

Substituting Eq. (10) we get

$$y_k = G (u_k + C (-y_k))$$

$$y_k = G u_k - G C (y_k)$$

$$y_k + G C (y_k) = G u_k$$

$$y_k (1 + G C) = G u_k$$

$$\frac{y_k}{u_k} = \frac{G}{1 + GC}$$

$$y_k = \frac{G}{1 + GC} u_k \quad \dots (11)$$

When the Eq. (11) is substituted into Eq. (10), then the error will be

$$e_k = \frac{-G}{1 + GC} u_k \quad \dots (12)$$

From Eq. (12), to find feed-forward signal U<sub>k</sub>

$$U_k = \frac{1 + GC}{-G} \times e_k \quad \dots (13)$$

Low-pass filter Q(s) = ω<sub>c</sub>/(s+ω<sub>c</sub>), where ω<sub>c</sub> is the cut-off frequency (rad/s), is chosen as the robustness filter (Q). Similar to this, ILC feed-forward loop determines the convergence rate of the false signal using the learning gain K<sub>l</sub>.

**Learning Update Rule**

From Fig. 4, the Learning update rule is derived as

$$u_{k+1} = Q. u_k + K.L.e_k \quad \dots (14)$$

Error iteration k+1 is derived by using the Eq. (12);

$$e_{k+1} = \frac{-G}{1+GC} u_{k+1} \quad \dots (15)$$

**Error Signal for the Next Run**

Subs, Eq. (14) in Eq. (15)

$$e_{k+1} = \frac{-G}{1+GC} Q u_k + L * \frac{-G}{1+GC} e_k \quad \dots (16)$$

Subs, Eq. (16) in Eq. (15) and it becomes,

$$e_{k+1} = \left( Q + \frac{-G}{1+GC} * L \right) e_k \quad \dots (17)$$

$$e_{k+1} = Q \left( 1 - \frac{1}{Q} * \frac{G}{(1+GC)} L \right) e_k$$

$$e_{k+1} = Q \left( 1 - \frac{1}{Q} * P_s L \right) e_k \quad \dots (18)$$

where, the process complimentary sensitivity;

$$P_s = \frac{G}{1+GC}$$

Error signal transmission from each iteration is depicted in Eq. (18). Convergence occurs when  $|Q(1 - P_s L)| < 1$ . A replacement of the learning filter L is  $P_s^{-1}$  i.e Responsiveness of inverted auxiliary process. where,  $P_s = \frac{G}{1+GC}$ , as a result, the reverse inter related responsiveness  $P_s^{-1}$  is unsuitable and unstable for use as a filter with the help of the ZPETC.<sup>7</sup> A discrete approximation for L is used to tackle this issue.<sup>7</sup> A discrete complementary sensitivity is inputted into the technique, which produces an unaltered stable discrete inverse complementary sensitivity. Then Eq. (18) has become,

$$e_{k+1} = Q(1 - k_l L \times P_s) e_k \dots (19)$$

If  $k_l=1$  and  $L = P_s^{-1}$ , Eq. (19) equals to zero. Flexibility against model flaws does not exist. If  $0 < k_l < 1$  is set, the convergence speed is reduced. Optimization method used in this work is used to calculate the learning gain that employs lowest tracking error as the objective function.

**Magnitude and Phase Plot**

Bode plot is displayed in Fig. 5. It is used to construct a robustness filter, cut-off frequency is found as 0.14 rad/s and ILC is incorporated with a proportional gain with the value of  $K_p = 0.5$ .

**PID Controller-Design and Implementation**

PID controller is employed in more than 95% of closed-loop industrial processes due to their

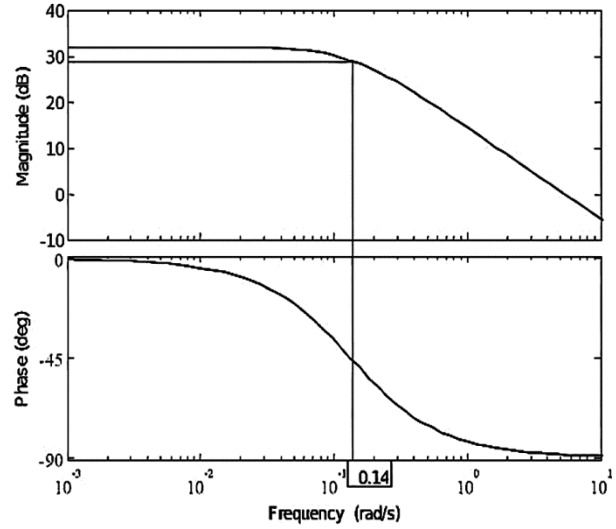


Fig. 5 — Magnitude and Phase of Bode plot

simplicity and outstanding performance in many applications. Unlike many other modern controllers, which are far more sophisticated but sometimes deliver only minimal improvement, it can be modified by operators with little or no experience with controls.<sup>34</sup>

The value of a robust controller is made evident when compared to conventional PID controllers. The transfer function is employed to determine the controller parameters. EHSS employs a PID controller to control the displacement of a double-acting hydraulic cylinder in response to an input signal. PID controller's proportional gain  $K_p$ , integral time  $T_i$  and derivative time  $T_d$  are calculated using Minimum IAE–Arrieta Orozco.<sup>35</sup>

$$K_p = \frac{0.2068 + 1.1597 \left( \frac{T_m}{\tau_m} \right)^{1.0158}}{K_m}$$

$$T_i = T_m \left( -0.2228 + 1.3009 \left( \frac{T_m}{\tau_m} \right)^{0.5022} \right)$$

$$T_d = 0.3953 T_m \left( \frac{T_m}{\tau_m} \right)^{0.8469}$$

**Graphical user Interface (GUI) of EHSS**

MATLAB Simulink is used to create the GUI displayed in Fig. 6. Controller block intend to control the system. Input block is utilized to deliver various inputs. The analog signal from the LVDT sensor senses the displacement of hydraulic cylinder and sends the signal to analog input block and the controller sends the signal to the analog output block based on the feedback signal. Movement of the piston is indicated by the output block.

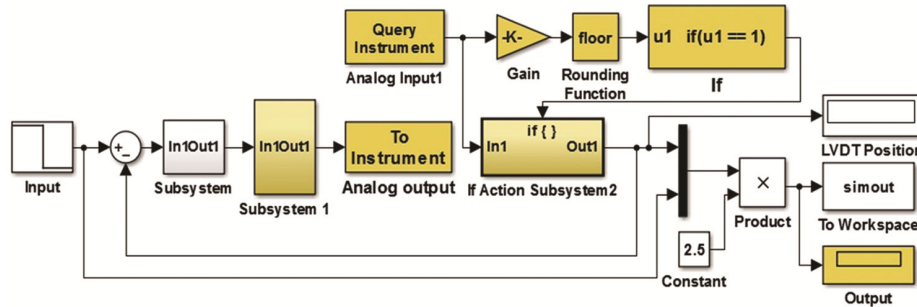


Fig. 6 — Graphical user interface of EHSS

**Results and Discussion**

Simulation and experimental responses of the square wave, set point tracking and servo responses were recorded to compare the performance of the ILC and PID controller.

**Servo Response**

The servo tracking is assessed individually for ILC and PID controller. Initially, the double-acting hydraulic cylinder is allowed to settle up to 50 sec at an intended position of 62.5 mm, 125 mm and 187.5 mm, which is 25%, 50% and 75% of the entire displacement (0–250 mm) then it undergoes a step change of  $\pm 10\%$ . The simulation responses are shown in Fig. 7 (a–c). The performance measures such as Maximum peak overshoot (Mp), Settling time (Ts) sec and Rise time (Tr) sec are recorded in Table 1. It's observed that ILC produces minimal overshoot of 0.2–0.6%, whereas PID controller has 1.3–3.6%. ILC has a quick settling time of 1.5 sec, but the PID controller settles at 6.2 sec. Rise time of both the controllers are almost similar, where rise time of the PID controller is 0.03 sec quicker than the ILC's. Experimental responses are shown in Fig. 8 (a–c) and their performance measures are tabulated in Table 2. ILC has a quick settling time of a minimum of 5 sec to a maximum of 23 sec lesser than PID controller. ILC has a less overshoot of 4–10%, whereas 10–45% observed in PID controller. Rise time of PID controller is 0.1–1 sec quicker than ILC. Error indices during simulation are tabulated in Table 3. PID has 10% lesser error indices (ISE and IAE) than the ILC, due to its better rise time response. Error indices during experimentation are recorded in Table 4 and it is found that PID has 11–36% of lesser error indices than the ILC.

**Square Wave Tracking**

The square wave tracking responses are observed with fixed amplitude of 125 with a varying pulse width of 50%, 75% and 100%. The results of square

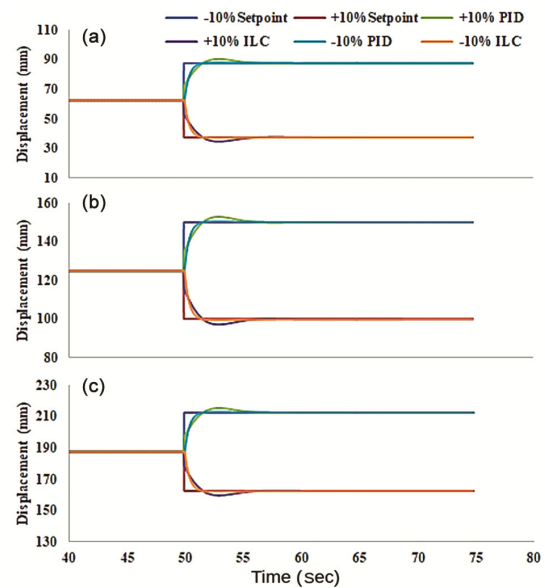


Fig. 7 — Simulation result of servo response at: (a) 62.5 mm, (b) 125 mm, (c) 187.5 mm

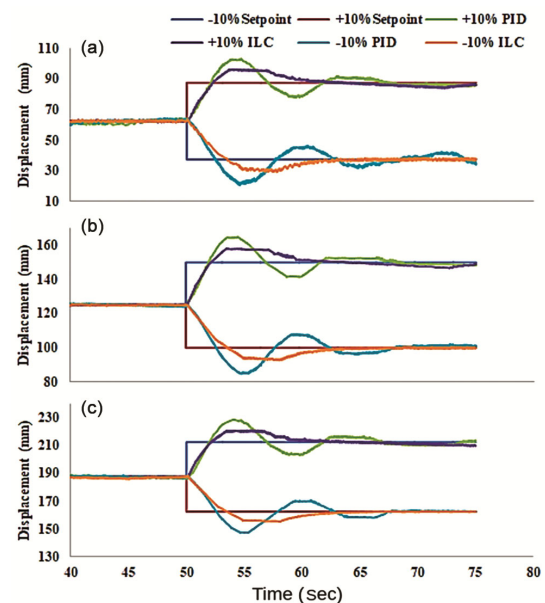


Fig. 8 — Experimental result of servo response at: (a) 62.5 mm, (b) 125 mm, (c) 187.5 mm

Table 1 — Performance comparison of servo response during simulation

Set point	Simulation					
	PID			ILC		
	Mp (%)	Ts (sec)	Tr (sec)	Mp (%)	Ts (sec)	Tr (sec)
62.5+10%	3.24	6.2	1.46	0.5	1.4	1.49
62.5-10%	3.6	6.2	1.46	0.6	1.4	1.49
125+10%	1.89	6.1	1.48	0.3	1.8	1.5
125-10%	2.85	6.2	1.49	0.45	1.5	1.49
187.5+10%	1.33	6.3	1.49	0.2	1.5	1.55
187.5-10%	1.74	6.2	1.49	0.3	1.5	1.53

Table 2 — Performance comparison of servo response during experimentation

Set point	Experimentation					
	PID			ILC		
	Mp (%)	Ts (sec)	Tr (sec)	Mp (%)	Ts (sec)	Tr (sec)
62.5+10%	17.8	17	2.11	10	10	2.31
62.5-10%	45.3	17	2.5	22.4	11	3.52
125+10%	29.5	17.5	1.95	5.4	10	2.14
125-10%	15.2	17.8	2.59	7.33	12	3.49
187.5+10%	17.6	17	2	4	09	2.1
187.5-10%	9.4	17.5	2.56	4.43	12	3.48

Table 3 — Error indices comparison of servo response during Simulation

Set point	Simulation			
	PID		ILC	
	ISE	IAE	ISE	IAE
62.5+10%	785.5	41.11	861.4	63.33
62.5-10%	785.5	41.11	861.4	63.33
125+10%	2818	70.49	3089	108.6
125-10%	2818	70.49	3089	108.6
187.5+10%	3206	99.89	3802	153.8
187.5-10%	3206	99.89	3802	153.8

Table 4 — Error indices comparison of servo response during experimentation

Set point	Experimental			
	PID		ILC	
	ISE	IAE	ISE	IAE
62.5+10%	8437	581.9	13270	685.1
62.5-10%	8578	595.4	13310	678.8
125+10%	21400	750.8	26180	836.7
125-10%	21550	741.7	26180	844.4
187.5+10%	35140	827	38830	1032
187.5-10%	35070	834.6	38970	1023

wave tracking responses in simulation are shown in Fig. 9 (a–c). PID has 10% overshoot mean while, ILC has zero overshoot at each cycle. Rise time of PID is 0.5 sec earlier than ILC and ILC settles at 5<sup>th</sup> sec whereas PID settles at 10<sup>th</sup> sec.

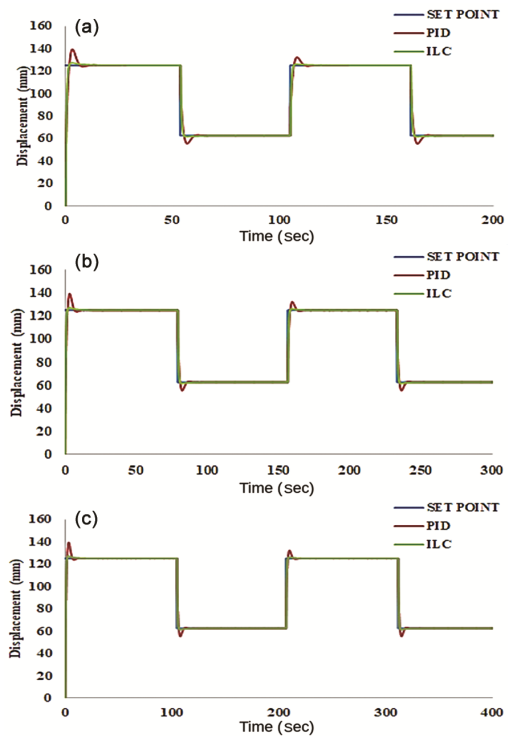


Fig. 9 — Simulation result of square wave response at: (a) 50% of pulse width, (b) 75% of pulse width, (c) 100% of pulse width

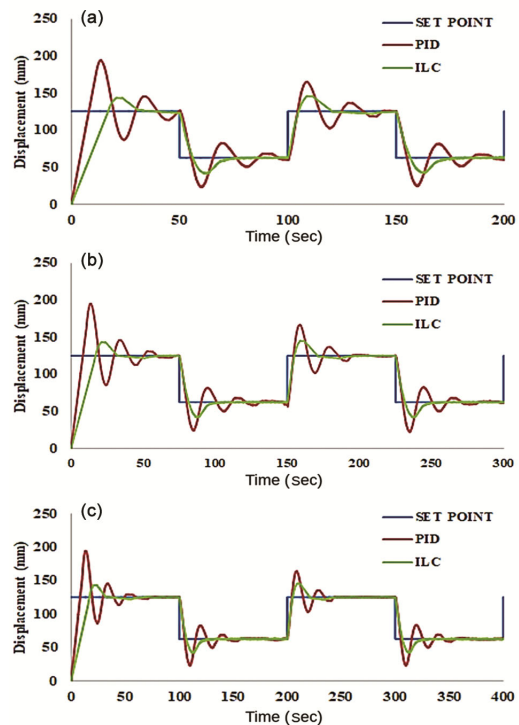


Fig. 10 — Experimental result of square wave response at: (a) 50% of pulse width, (b) 75% of pulse width, (c) 100% of pulse width

The results of square wave tracking responses at experimentation are shown in Fig. 10 (a–c). At 50%

of pulse width, PID controller has failed to settle within the time period. At 75% and 100% of pulse width, PID controller response settles just before the first half cycle. Meanwhile, ILC performs more admirably than the PID controller in tracking the square wave form, it settles quickly for all the periods of the pulse width. PID has 52% overshoot but ILC has only 12%.

The error indices are tabulated in Table 5. In simulation, PID suppresses ISE than ILC by 8% at 50%, 75% and 100% period of pulse width respectively. During experimentation, 3.3%, 1.6%, and 3.8% at 50%, 75%, and 100% period of pulse width is observed. In simulation, ILC produces more IAE than PID by 35%. Experimental results show the increase of 25%, 27%, and 25% at 50%, 75%, and 100% period of pulse width respectively.

**Set Point Tracking**

Set point tracking analysis demonstrates the controller's efficiency in the presence of changes in various set points over a period of time. The set point and time intervals of input signals are chosen randomly. The simulation result is shown in Fig. 11 a. ILC has 1–2%, where as PID has 6–11% overshoot,

settling time of ILC is below 1 sec and PID controller takes 3 sec. Both the controller has similar rise time responses.

From the experimental result shown in Fig. 11 b, it's observed that ILC has 10–28% overshoot and PID has an overshoot of 30–50%. Settling time of ILC is 20–30sec, whereas the PID controller settles at 40–52 sec. Set point variation increases over the period of time. The error indices comparison is tabulated in Table 6. PID suppresses the ISE than ILC by 8% in simulation and 13% in the experimental results. ILC has a larger IAE than PID by 35% in simulation and 22% in the experimental results. Overshoot and settling time increases, when the variation of the input is higher.

To test the effectiveness of the proposed controller, SMC is compared with it. For comparison, the square wave response is simulated and it is displayed in Fig. 12. Similar responses are obtained in both controllers. To illustrate the effectiveness of ILC, error indices such as ISE and IAE are compared in Table 7. From the Table 7, it is evident that ILC has 56% lesser ISE and 23% higher IAE. From this comparison, it is deliberate that both the controllers are intelligent enough to overcome the nonlinearity and imprecision

Table 5 — Error indices comparison of the square wave tracking

Pulse Width (%)	Para meter	Simulation		Experimentation	
		PID	ILC	PID	ILC
50	ISE	4742	5198	29600	30580
	IAE	146.9	226.1	1119	1499
75	ISE	4742	5198	30320	30830
	IAE	146.9	226.1	1153	1593
100	ISE	4742	5198	29610	30780
	IAE	146.9	226.1	1167	1563

Table 6 — Error Indices comparison of set point tracking response

Controller	Simulation		Experimentation	
	ISE	IAE	ISE	IAE
PID	1355	58.89	30820	1759
ILC	1482	90.48	35570	2245

Table 7 — Error Indices comparison of square wave response of ILC and SMC

Controller	Simulation	
	ISE	IAE
ILC	7196	216.6
SMC	12890	175.8

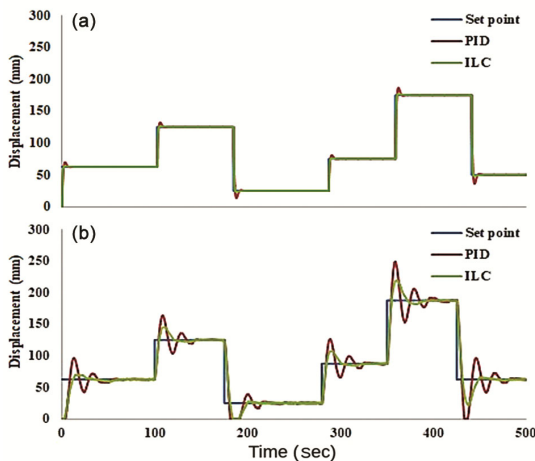


Fig. 11 — Set point tracking: (a) simulation result, (b) experimental result

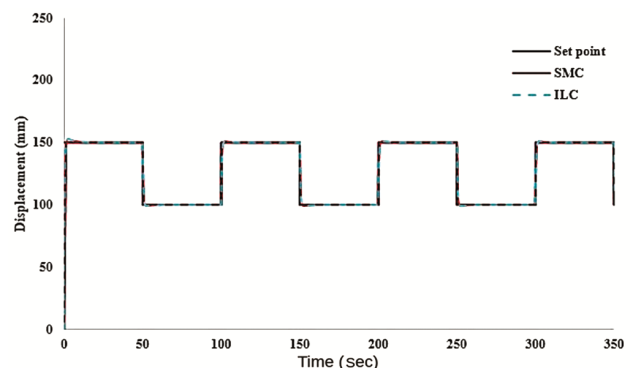


Fig. 12 — Simulation result of square wave response of ILC and SMC at 50% of pulse width

that occurs in the hydraulic systems because of friction.

## Conclusions

The piston displacement of a hydraulic cylinder is controlled in this study using an ILC. The variation in time and time domain parameters in simulation and experimentation results are because of the nonlinearities and uncertainties of the system. ILC performs better than PID controllers in vital areas including notably quick settling time and lower overshoot. This exhibits the ILC's robustness and shows how the ILC technique can handle industrial hydraulic press applications that are nonlinear and unpredictable. The limitation of the proposed ILC is higher rise time and error indices as compared with PID controller, which is mainly due to model uncertainties. In future the proposed controller can be implemented in real time industrial hydraulic applications to test the feasibility of the controller.

## Reference

- 1 Tony T A, Parameshwaran R, Sathiyavathi S & Vimala S A, Improved position tracking performance of electro hydraulic actuator using PID and sliding mode controller, *IETE J Res*, **68(3)** (2019) 1683–1695.
- 2 Lee C, Jeon C W, Han X, Kim J H & Kim H J, Application of electrohydraulic proportional valve for steering improvement of an autonomous tractor, *J Biosyst Eng*, **47** (2022) 167–180.
- 3 Rodriguez G D, Favela C A, Beltrann C F, Sotelo C & Sotelo D, An MPC-LQR-LPV controller with quadratic stability conditions for a nonlinear half-car active suspension system with electro-hydraulic actuators, *Mach*, **10(2)** (2022) 137.
- 4 Zhang Z, Wang B, Ma T & Ai B, Fuzzy decoupling predictive functional control for nonlinear hydro-turbine governing systems with mechanical time delay of the hydraulic servo system, *J Vibrat Control*, **29(5–6)** (2022) 1292–1306, <https://doi.org/10.1177/10775463211062332>.
- 5 Zheng J M, Zhao S D & Wei S G, Fuzzy iterative learning control of electro-hydraulic servo system for SRM direct-drive volume control hydraulic press, *J Cent South Univ Technol*, **17(2)** (2010) 316–322.
- 6 Dwyer O A, *Handbook of PI and PID controller tuning rules* (World Scientific) 2009.
- 7 Wang X J, Li J Y, Wu B & Shao J P, Continuous rotary motor electro-hydraulic servo system based on the zero phase error tracking controller, *Appl Mech Mater*, **121** (2012) 3205–3209.
- 8 Di G E, Santelia M, Bruni S & Zolotas A, A simple active carbody roll scheme for hydraulically actuated railway vehicles using internal model control, *ISA Trans*, **120** (2022) 55–69.
- 9 Shi Q & He L, A model predictive control approach for electro-hydraulic braking by wire, *IEEE Trans Ind Info*, **19(2)** (2022) 1380–1388.
- 10 Dalwadi N, Deb D & Muyeen S M, Adaptive backstepping controller design of quadrotor biplane for payload delivery, *IET Intell Transp Syst*, **6(12)** (2022) 1738–1752.
- 11 Shaojuan Y & Junjun S, Iterative learning control of double servo valve controlled electro hydraulic servo system, *7<sup>th</sup> Int Conf Comput Intell Secur* (Sanya, China) 2011, 278–282, doi: 10.1109/CIS.2011.69.
- 12 Moonumca P, Depaiwa N & Yamamoto Y, Tuning PID controller using genetic algorithms for electro-hydraulic system with tracking force control, *Adv Mater Res*, **931** (2014) 1318–1322.
- 13 Dahunsi O, Pedro J & Nyandoro O, System identification and neural network based PID control of servo-hydraulic vehicle suspension system, *SAIEE Afr Res J*, **101(3)** (2010) 93–105.
- 14 Moon B Y, Study of parameter identification using hybrid neural-genetic algorithm in electro-hydraulic servo system, *ICMIT 2005 Cont Syst Robot* (International Society for Optics and Photonics) 2006, 60422G-1.
- 15 Aly A A, PID parameters optimization using genetic algorithm technique for electrohydraulic servo control system, *Intell Cont Autom*, **2(02)** (2011) 69.
- 16 Guo Q, Shi G, Wang D, He C, Hu J & Wang W, Iterative learning based output feedback control for electro-hydraulic loading system of a gait simulator, *Mechatron*, **54** (2018) 110–120.
- 17 Shen D, Iterative learning control with incomplete information, *IEEE/CAA J Autom Sin*, **5(5)** (2018) 885–901.
- 18 Zhuang Z, Tao H, Chen Y, Stojanovic V & Paszke W, Iterative learning control for repetitive tasks with randomly varying trial lengths using successive projection, *Int J Adapt Control Signal Process*, **36(5)** (2022) 1196–1215.
- 19 Bristow D A, Tharayil M & Alleyne A G, A survey of iterative learning control, *IEEE Control Syst Mag*, **26(3)** (2006) 96–114.
- 20 Freeman C T, Hughes A M, Burrige J H, Chappell P H, Lewin P L & Rogers E, Iterative learning control of FES applied to the upper extremity for rehabilitation, *Control Eng Pract*, **17(3)** (2009) 368–381.
- 21 Lim I, Hoelzle D J & Barton K L, A multi-objective iterative learning control approach for additive manufacturing applications, *Cont Eng Pract*, **64** (2017) 74–87.
- 22 Dong-II Kim M & Sungkwun Kim, An iterative learning control method with application for CNC machine tools, *IEEE Trans Ind Appl*, **32(1)** (1996) 66–72.
- 23 Pandit M, Buchheit K H, Furong Gaoa & Yi Yanga C S, Optimizing iterative learning control of cyclic production processes with application to extruders, *IEEE Trans Control Syst Tech*, **7(3)** (1999) 7025–7034.
- 24 Cheng Peng L S, Wenlong Zhang & Masayoshi Tomizuka, Optimization-based constrained iterative learning control with application to building temperature control systems, *IEEE Int Conf Adv Intell Mechatron*, (IEEE) 2016, 709–715.
- 25 Mezghani M, Roux G, Cabassud M, Le Lann M V, Dahhou B & Casamatta G, Application of iterative learning control to an exothermic semibatch chemical reactor, *IEEE Trans Control Syst Tech*, **10(6)** (2002) 822–834.
- 26 Sahoo S K, Panda S K & Xu J X, Iterative learning-based high-performance current controller for switched reluctance motors, *IEEE Trans Power Appar Syst*, **19(3)** (2004) 491–498.

- 27 Zhao S, Wang J, Wang L, Hua C & He Y, Iterative learning control of electro-hydraulic proportional feeding system in slotting machine for metal bar cropping, *Int J Mach Tools Manuf*, **45(7–8)** (2005) 923–931.
- 28 Ratcliffe J D, Lewin P L, Rogers E, Hatonen J J & Owens D H, Norm-Optimal iterative learning control applied to gantry robots for automation applications, *IEEE Trans Rob*, **22(6)** (2006) 1303–1307.
- 29 Boudjedir C E, Bouri M & Boukhetala D, Model-free iterative learning control with nonrepetitive trajectories for second-order MIMO nonlinear systems-Application to a delta robot, *IEEE Trans Ind Electron Control Instrum*, **68(8)** (2020) 7433–7443.
- 30 Jin X, Fault-tolerant iterative learning control for mobile robots non-repetitive trajectory tracking with output constraints, *Autom*, **94** (2018) 63–71.
- 31 Yu S, Bai J, Xiong S & Han R, A new iterative learning controller for electro-pneumatic servo system, *8<sup>th</sup> Int Conf Intell Syst Design Appl*, **3** (2008) 101–105.
- 32 Sandipan M J C & Tomizuka M, Precision positioning of wafer scanners segmented iterative learning control for nonrepetitive disturbances, *IEEE Control Syst Mag*, **27(4)** (2007) 20–25.
- 33 Li X D, Lv M M & Ho J K L, Adaptive ILC algorithms of nonlinear continuous systems with non-parametric uncertainties for non-repetitive trajectory tracking, *Int J Syst Sci*, **47(10)** (2015) 2279–2289.
- 34 Astrom K J & Hagglund T, New tuning methods for PID controllers, in *European Control Conf* 1995.
- 35 Arrieta O, *Tuning of PI & PID Controllers using a Multi Criteria Performance Index*, Ph.D. dissertation, University of Costa Rica, 2006.